scientific reports

Check for updates

OPEN

Vorinostat attenuates UVB-induced skin senescence by modulating NF-κB and mTOR signaling pathways

Qianlong Dai[1,3], Zhiwei Wang[1,3], Xue Wang[2,3], Wei Lian[1], Yuchen Ge[1], Shujia Song[1], Fuxing Li[1], Bingxiang Zhao[1], Lihua Li[2], Xiaobo Wang[1]✉, Min Zhou[1]✉ & Jianjie Cheng[2]✉

Excessive exposure to ultraviolet B (UVB) radiation induces oxidative stress and inflammatory responses, accelerating the senescence process of skin cells. Vorinostat (SAHA), a histone deacetylase inhibitor (HDACi), is typically administered to patients with peripheral T-cell lymphoma, cutaneous T-cell lymphoma, or multiple myeloma. However, its effect on UVB-induced skin photoaging remains unclear. In this study, we used UVB to induce senescence in human immortalized keratinocyte cell line (HaCaT cells) and skin photoaging in Balb/c mice to investigate the potential of SAHA in mitigating photoaging. First, we established a UVB-induced photoaging model in HaCaT cells. We observed that UVB exposure significantly upregulated the activity of senescence-associated β-galactosidase, p16, p21, IL-1β, IL-6, and matrix metalloproteinases [collagenase (MMP-1), matrix metalloproteinase-3 (MMP-3), and gelatinase (MMP-9)]. Supplementation with SAHA effectively alleviated cellular senescence in HaCaT cells. Next, we used UVB to induce photoaging in Balb/c mouse skin. The study demonstrated that UVB markedly caused skin senescence in Balb/c mice, while SAHA effectively mitigated the changes induced by UVB irradiation. Mechanistically, we found that UVB activated the mammalian target of rapamycin (mTOR) and nuclear factor-κB (NF-κB) signaling pathways, whereas SAHA inhibited the upregulation of both mTOR and NF-κB. In summary, these findings suggest that SAHA may protect against UVB-induced cellular senescence and skin photoaging by inhibiting the mTOR and NF-κB signaling pathways. Therefore, SAHA could be a potential anti-senescence agent for mitigating skin photoaging.

Keywords Vorinostat, UVB-induced, Anti-photoaging, mTOR, NF-κB

The skin is the largest organ of the human body, composed of the epidermis, dermis, and subcutaneous tissue. It not only protects the body from physical, chemical, and microbial damage but also senses mechanical stimuli, pain, and temperature changes[1,2]. In recent years, environmental degradation has led to the depletion of the ozone layer, resulting in a sharp increase in UVB radiation intensity. Excessive UVB radiation can cause various skin diseases, such as sunburn, photoaging, irregular pigmentation, and skin cancer[3,4]. UVB radiation induces the production of reactive oxygen species (ROS), leading to DNA, protein, and lipid damage, as well as the production of inflammatory cytokines[5,6]. This activates various signaling pathways, resulting in cellular structural collapse and the accumulation of oxidative stress within cells, ultimately causing photoaging[1,7–9]. Skin senescence is primarily characterized by the loss of skin structure and physiological functions, and it can be categorized into intrinsic senescence and extrinsic senescence[10,11]. Intrinsic senescence is typically associated with reduced synthesis of biological proteins and decreased hormone secretion. In contrast, extrinsic senescence, caused by air pollution and UVB-induced photoaging, significantly accelerates the skin senescence process[12–14]. The characteristics of photoaged skin include epidermal thickening and degradation of elastic fibers[9]. Additionally, UVB exposure can cause DNA damage and protein structure disruption in skin cells, leading to wrinkles, inflammation, and cancer[15]. Recent studies have shown that certain compounds, such as polyphenols, retinyl palmitate, and hydroquinone, can improve the symptoms of skin senescence. However, these compounds are often expensive and have side effects, such as skin irritation and allergic reactions[13]. Therefore, finding safe and effective alternative drugs to improve photoaging of the skin is of particular importance.

UVB-induced photoaging of the skin leads to DNA damage and activates inflammatory cytokines, which in turn activate various signaling pathways, resulting in skin damage and senescence[16,17]. Specifically, DNA

[1]School of Basic Medicine, Dali University, Dali 671000, Yunnan, China. [2]Department of Neurosurgery, The First Affiliated Hospital of Dali University, Dali 671000, Yunnan, China. [3]Qianlong Dai, Zhiwei Wang and Xue Wang contributed equally to this work. ✉email: wxb4320062@163.com; may-zhoumin@163.com; dljch@163.com

damage activates the ATM/ATR kinases and the p53/p21/CIP1 signaling axis[18]. p53 is a crucial participant in the DNA damage response (DDR), preventing uncontrolled cell growth and division, and inducing signaling through several downstream effector arms. Among these, p21 is one of the important targets of p53[19]. As a cyclin-dependent kinase (CDK) inhibitor, p21 plays a key role in regulating the G1/S checkpoint, causing cell cycle arrest. Persistent damage may ultimately lead to cellular senescence[20]. Characteristics of cellular senescence include cell cycle arrest, expression of the senescence-associated secretory phenotype (SASP), accumulation of p16INK4a, and activation of the mTOR signaling pathway[21]. mTOR is an evolutionarily conserved serine/threonine kinase that integrates various extracellular and intracellular signals to maintain cellular homeostasis and metabolism. Aberrant activation of the mTOR signaling pathway is one of the key mechanisms leading to senescence[22–25]. Moreover, UVB promotes the secretion of various MMPs, particularly the overexpression of MMP-1, MMP-3, and MMP-9, which contribute to the degradation of type I collagen, leading to the destruction of the dermal and skin structure[26,27]. Concurrently, UVB upregulates pro-inflammatory cytokines such as TNF-αand IL-6, activating the oxidative stress-sensitive NF-κB pathway. This further upregulates MMP-9 expression, ultimately contributing to the occurrence of photoaging[28,29].

Vorinostat (suberoylanilide hydroxamic acid, SAHA) is a pan-HDAC (class I and II) inhibitor approved by the U.S. Food and Drug Administration (FDA) primarily for the treatment of advanced refractory cutaneous T-cell lymphoma[30]. As a chelator of the zinc ion in the active site of histone deacetylases (HDACs), SAHA is considered a promising anticancer chemotherapeutic agent. By inhibiting HDAC, SAHA blocks the deacetylation of histones, thereby altering chromatin structure and relieving transcriptional repression[31]. HDACs have been identified as potential drug targets for numerous diseases, including various cancers, fibrotic diseases, autoimmune and inflammatory diseases, and metabolic disorders[32,33]. However, reports on the role of SAHA in protecting the skin from UVB-induced photoaging are relatively limited.

This study aims to investigate the anti-senescence potential and underlying mechanisms of SAHA in UVB-induced cellular and animal models. Initially, a HaCaT cell model was established to evaluate the alleviating effects of SAHA on UVB-induced cellular senescence and to screen potential associated signaling pathways. Subsequently, the therapeutic effects of SAHA were further validated in a UVB-induced photoaging model in the dorsal skin of BALB/c mice. Through these experiments, we aim to elucidate the potential mechanisms by which SAHA exerts its anti-senescence effects, providing novel therapeutic strategies for UVB-induced skin photoaging.

Materials and methods

Chemicals and reagents

Vorinostat (SAHA) (S1047) was purchased from Selleck Chemicals (Shanghai, China). Hematoxylin–Eosin staining kit (Cat# G1120) was obtained from Solarbio (Beijing, China). Senescence-associated β-galactosidase (SA-β-Gal) Stain Kit (Cat# G1580) was purchased from Solarbio (Beijing, China). Trypsin EDTA digestion solution (T1300), L-Glutamine (G0200), and mixed solution of penicillin (P1400) were purchased from Soraibao (Beijing, China). FBS (C04011) was purchased from Via Cell (Shanghai, China). Insulin (S6955) were supplied by Selleck (Shanghai, China). 100% dimethyl sulfoxide (DMSO) (D8371) was purchased from Solarbio (Beijing, China). Mem medium (PM150410) was bought from Pricella (Wuhan, China), SweScript All-in-One First-Strand cDNA Synthesis SuperMix for qPCR (G3337-50), and 2× SYBR Green qPCR Master Mix (G3326-1) were procured from Servicebio (Wuhan, China). Trizol Reagent (CW0580) was purchased from Cwbio (Jiangsu China). Cell Counting Kit-8 reagent (Cat# PF00004), HRP conjugated Goat Anti-Mouse IgG (H + L) (Cat#GB23301, 1:10,000) and HRP conjugated Goat Anti-Rabbit IgG (H + L) (Cat#GB23303, 1:10,000) were purchased from Servicebio (Wuhan, China). Antibody against GAPDH (Cat#ab181602, 1:2000) was purchased from Abcam (Shanghai, China). Anti-Rabbit-MMP1 (10371-2-AP, 1:1000), Anti-Rabbit-MMP3 (17873-1-AP, 1:1000) and Anti-Rabbit-MMP9 (10371-2-AP, 1:1000) were purchased from Proteintech (Wuhan, China). Phospho-P38 MAPK (Thr180/Tyr182) Rabbit mAb (Cat #4511, 1:1500) and Phospho-NF-κB p65 (Ser536) (93H1) Rabbit mAb (Cat#3033 1:1500) were purchased from Cell Signaling Technology (Danvers, MA, United States). P16 (Cat#SR34-02, 1:1000) was purchased from Huabio (Hangzhou, China). Phospho-mTOR (Ser2448) (Cat#5536, 1:1000) was purchased from Cell Signaling Technology (Danvers, MA, United States). A Scientz03-II UV radiation system (312 nm, 60 W) (Xinzhi, Ningbo, China).

Cell culture

First, a complete medium containing 86% MEM medium (PM150410) (Pricella, Wuhan, China), 1% L-glutamine, 1% Penicillin–Streptomycin Solution, and 12% FBS was used. HaCaT cells (CL-0090, Procell, Wuhan, China) were cultured in 6-cm dishes using 4 ml of the complete medium. The cells were digested in Trypsin–EDTA solution, 0.25% (Cat# T1300) (Solarbio, Beijing, China) for 7 min. The complete medium was added to terminate the digestion. The cells were centrifuged for 5 min at 1100 rpm, incubated at 37 °C with 5% CO_2, and passaged every 48 h.

UVB-induced senescence of HaCaT cells

In this study, HaCaT cells were divided into three groups: the control group, the model group, and the SAHA group. The control group received no treatment. Prior to UVB irradiation, the culture medium was completely removed from the culture dishes. To ensure uniform irradiation and eliminate potential interference from medium components, the cells were gently rinsed twice with phosphate-buffered saline (PBS) to remove any residual medium and metabolic byproducts. During irradiation, a thin layer of PBS was maintained on the cell surface to prevent dehydration, as PBS exhibits minimal UVB absorption.

Studies have shown that UVB irradiation at 30–60 mJ/cm^2 effectively induces photoaging in HaCaT cells, with 40 mJ/cm^2 and 50 mJ/cm^2 widely validated for successfully modeling UVB-induced photodamage[34–37].

Furthermore, in our previous study, a comparison between single high-dose and dual low-dose UVB regimens revealed that the 40 mJ/cm^2 (day 1) + 50 mJ/cm^2 (day 2) combination most effectively induced SA-β-gal positivity while minimizing cytotoxicity[20,34]. Additionally, preliminary experiments further confirmed that this regimen robustly induced senescence-associated phenotypes with high reproducibility. Therefore, the 40 mJ/cm^2 + 50 mJ/cm^2 UVB exposure protocol was adopted in this study.

Furthermore, to ensure the accurate and uniform delivery of the designated UVB doses (40 mJ/cm^2 on the first day and 50 mJ/cm^2 on the second day), the culture dish lids were removed during irradiation to prevent any potential absorption or reflection effects. In the model group, the cells were exposed to UVB at 40 mJ/cm^2 and 50 mJ/cm^2 on the first and second days, respectively. In the SAHA group, following UVB irradiation, the cells were treated with SAHA. Subsequently, at 24 and 48 h post-irradiation, key indicators related to photoaging, inflammation, and cellular damage were analyzed.

Drug

Vorinostat (SAHA) (S1047, Selleck, Shanghai, China) was dissolved in 100% dimethyl sulfoxide (DMSO, Solarbio, Beijing, China) to prepare a 50 mM stock solution, aliquoted, and stored at − 80 °C. For in vitro assays, working concentrations (1–10 μM) were prepared by diluting the stock solution in complete cell culture medium, ensuring a final DMSO concentration of ≤ 0.1% (v/v).

Insulin (S6955, Selleck, Shanghai, China) was dissolved in sterile 0.01 M hydrochloric acid (HCl) to prepare a 50 mM stock solution. For mTOR pathway activation, cells were treated with 10 nM insulin, prepared by diluting the stock solution in serum-free medium.

Cell viability test

In order to test cell viability, HaCaT cells were cultured at a density of 10,000 cells per well in 96-well plates containing 100 μl of complete medium. The experimental groupings are as described above in "UVB-induced senescence of HaCaT cells" section. First, the optical density (OD) of HaCaT cells treated with varying concentrations of SAHA was measured after 48 h. Cells without the drug served as the control group. Subsequently, the OD of the control vehicle group, the model group, and the SAHA groups with varying concentrations were tested at 48 h. At the testing time, 90% complete culture medium was mixed with 10% CCK-8 reagent and added to the cells in 96-well plates. The OD was evaluated to determine cell viability. The experiment was repeated three times, with three replicates each time.

Animals

In this study, 18 male BALB/c mice (10 weeks old) were obtained from Hunan Silaikejingda Experimental Animal Co., Ltd. (Changsha, China). The mice were housed under specific-pathogen-free (SPF) conditions at a controlled environment with a temperature of 23 ± 2 °C, relative humidity of 60%, and a 12-h light/dark cycle. They had free access to standard laboratory chow and sterile water. All experimental protocols were approved by the Animal Protection and Ethics Committee of Dali University (IACUC 2022-P2-21, Dali, Yunnan, China). All the methods were performed in accordance with the relevant guidelines and regulations. To minimize potential stress and movement during UVB irradiation, the mice were anesthetized by intraperitoneal injection of sodium pentobarbital (100 mg/kg) prior to exposure, ensuring consistent irradiation to the dorsal skin. After anesthetization, the back hair was removed using depilatory cream before the UVB exposure. The mice were randomly assigned to three groups (n = 6 per group): Sham group (PBS treatment), UVB group (750 mJ/cm^2 UVB exposure), and SAHA group (750 mJ/cm^2 UVB exposure followed by treatment with 150 μl of 10 mM SAHA solution). On day 6, the mice were humanely euthanized under deep anesthesia induced by sodium pentobarbital (100 mg/kg, intraperitoneal), followed by cervical dislocation to ensure death. Skin tissue samples were then collected for further molecular and histological analysis.

Histological analysis

The skin tissues were rapidly frozen and fixed using an embedding agent. Subsequently, they were sectioned into 8 μm slices. These sections were stained with hematoxylin–eosin (HE), SA-β-Gal, and Masson's trichrome. HE staining kits were used to assess skin thickness in mice according to the manufacturer's instructions. Sections stained with Masson's trichrome were used to assess collagen fibers and were observed under a microscope as per the protocol. SA-β-Gal staining kits were used to assess the activity of SA-β-Gal. All methods were carried out in accordance with the reference methods cited above.

SA-β-Gal stain

The SA-β-Gal staining kit was used to determine the activity of SA-β-Gal at specific time points in cells and tissues. After washing once with PBS, the cells were fixed for 15 min at room temperature with a fixative. Subsequently, the cells were washed three times with PBS, each wash lasting 3 min. The 8 μm tissue sections were washed once with PBS and fixed with a fixative for 25 min at ambient temperature. The sections were then gently washed three times with PBS for 5 min each. The tissues were subsequently immersed in the SA-β-Gal staining solution and incubated at 37 °C for 48 h.

Immunoblotting

After processing the cell and animal samples, the protein content was detected using Western blotting. First, total protein from the cells or tissues was extracted using RIPA buffer. The protein concentration was then determined using the BCA Protein Assay Kit (Cat# PC0020) (Solarbio, Beijing, China). Electrophoresis was performed after adding sodium dodecyl sulfate (SDS) loading buffer and boiling the samples for 10 min. The proteins were subsequently transferred onto a polyvinylidene fluoride (PVDF) membrane (Cat# Pall_BSP0161)

(Bio-Rad, Shanghai, China), which was blocked with milk (5% skim milk) and incubated overnight at 4 °C with the corresponding primary antibody. The membrane was then washed with Tween-20 phosphate-buffered saline (TPBS) and incubated with a secondary antibody (diluted 1:10,000) for 1 h at room temperature on a shaker. The bands were visualized using electrochemiluminescence, and band intensities were quantified using ImageJ analysis software.

Real-time PCR analysis

Total RNA was extracted from the cells and mouse skin tissues using TRIzol reagent (Takara, Shiga, Japan). The RNA was then reverse transcribed into cDNA. For qPCR analysis, 1 μg of cDNA was used, with GAPDH or 18S rRNA as a control. The cycle threshold (CT) values were compared to determine the relative levels of cDNA. PCR primers for mouse and human genes were obtained from Qingdao Biotech (Table S1).

Statistical analysis

The differences between the treatment groups were compared using the Student's t-test. One-way ANOVA was used to assess variance, followed by Bonferroni post hoc testing to evaluate differences between groups. A p value < 0.05 was considered statistically significant, $p < 0.01$ was considered moderately significant, and $p < 0.005$ was considered highly significant. Statistical analyses were performed on data from at least three independent experiments, and the results are presented as means ± SD.

Data availability

The data that support the findings of this study are available from the corresponding author upon reasonable request.

Result

SAHA alleviated UVB-induced senescence in HaCaT cells

To evaluate the anti-senescence effect of SAHA supplementation on UVB-induced senescence in HaCaT cells, we measured the expression levels of SA-β-gal, one of the most commonly used markers for detecting cellular senescence. The results showed that in the control group, SA-β-gal positive cells were less than 5%. In the UVB group, SA-β-gal positive cells significantly increased to over 60%. In the SAHA treatment group, with increasing doses of SAHA, the percentage of SA-β-gal positive cells significantly decreased, approaching a level similar to the control group, around 5% (Fig. 1a,b). Subsequently, we assessed cell viability at different concentrations of SAHA. The results indicated that starting from 1 μM, there was a decline in cell viability, suggesting a notable cytotoxic effect (Fig. 1c). Research has shown that UVB-induced photoaging can lead to reduced cell viability, delayed cell proliferation, and other cellular issues. Therefore, we further examined the impact of SAHA on HaCaT cell viability under UVB radiation. The findings demonstrated that as the UVB radiation intensity increased, cell viability gradually decreased. Notably, supplementation with 1 μM SAHA mitigated the UVB-induced reduction in cell viability (Fig. 1d). Based on the SA-β-gal staining results and cell viability assays, we ultimately selected 1 μM SAHA as the optimal concentration for subsequent studies. Since senescent cells typically express high levels of the proteins p16, p53, and p21, we utilized Western blotting and qPCR to assess the expression of these proteins and their corresponding genes in HaCaT cells induced by UVB over different time points. We found that compared to the control group, the level of p16 protein in the UVB group slightly increased at 24 h and significantly increased at 48 h. In contrast, in the SAHA-treated group, the p16 protein level significantly decreased at 48 h (Fig. 1e,f). Additionally, qPCR results showed that the mRNA expression levels of p53 and p21 were significantly higher in the UVB group compared to the control group. However, in the SAHA-treated group, the mRNA expression levels of p53 and p21 were significantly suppressed (Fig. 1g,h). Collectively, these results suggest that SAHA has a promising effect in alleviating UVB-induced photoaging in HaCaT cells.

SAHA inhibits the UVB-induced mTOR signaling pathways

In Fig. 1, we observed that SAHA alleviated the expression of senescence biomarkers (SA-β-gal, p16, p53, and p21), thereby mitigating UVB-induced photoaging in HaCaT cells. Next, we explored the mechanism by which SAHA alleviates photoaging in HaCaT cells. Research has shown that the mTOR pathway plays a crucial role in the regulation of senescence. Therefore, we assessed the expression levels of mTOR protein using Western blotting. The results indicated that the expression of phosphorylated mTOR (p-mTOR) was higher in the UVB group compared to the control group. In contrast, the SAHA-treated group exhibited a significant reduction in p-mTOR expression compared to the UVB group (Fig. 2a–c). Interestingly, when a specific mTOR chemical activator, insulin, was present, the percentage of SA-β-gal positive cells in the insulin-treated group significantly increased by over 30%, and the anti-senescence effect of SAHA was notably reduced (Fig. 2e,f). Subsequently, we measured the phosphorylation level of mTOR protein. In the insulin-treated group, insulin restored mTOR phosphorylation, resulting in elevated p-mTOR protein levels (Fig. 2b–d). These findings suggest that SAHA mitigates UVB-induced photoaging by reducing mTOR activity.

SAHA inhibit UVB-induced inflammatory responses in HaCaT cells

Senescent cells and tissues tend to secrete a large number of pro-inflammatory cytokines, activating the NF-κB signaling pathway. Additionally, excessive UVB exposure to skin cells generates a significant amount of intracellular reactive oxygen species (ROS), which can lead to an inflammatory cascade response in photoaging, such as the tumor necrosis factor-α (TNFα)-induced inflammatory pathway via activation of nuclear factor-κB (NF-κB). Inflammation is both a trigger and a marker of photoaging. Therefore, we assessed the expression levels of NF-κB protein in HaCaT cells using Western blotting. We found that the expression level of phosphorylated NF-κB protein was significantly higher in the UVB group compared to the control group. In the SAHA-treated

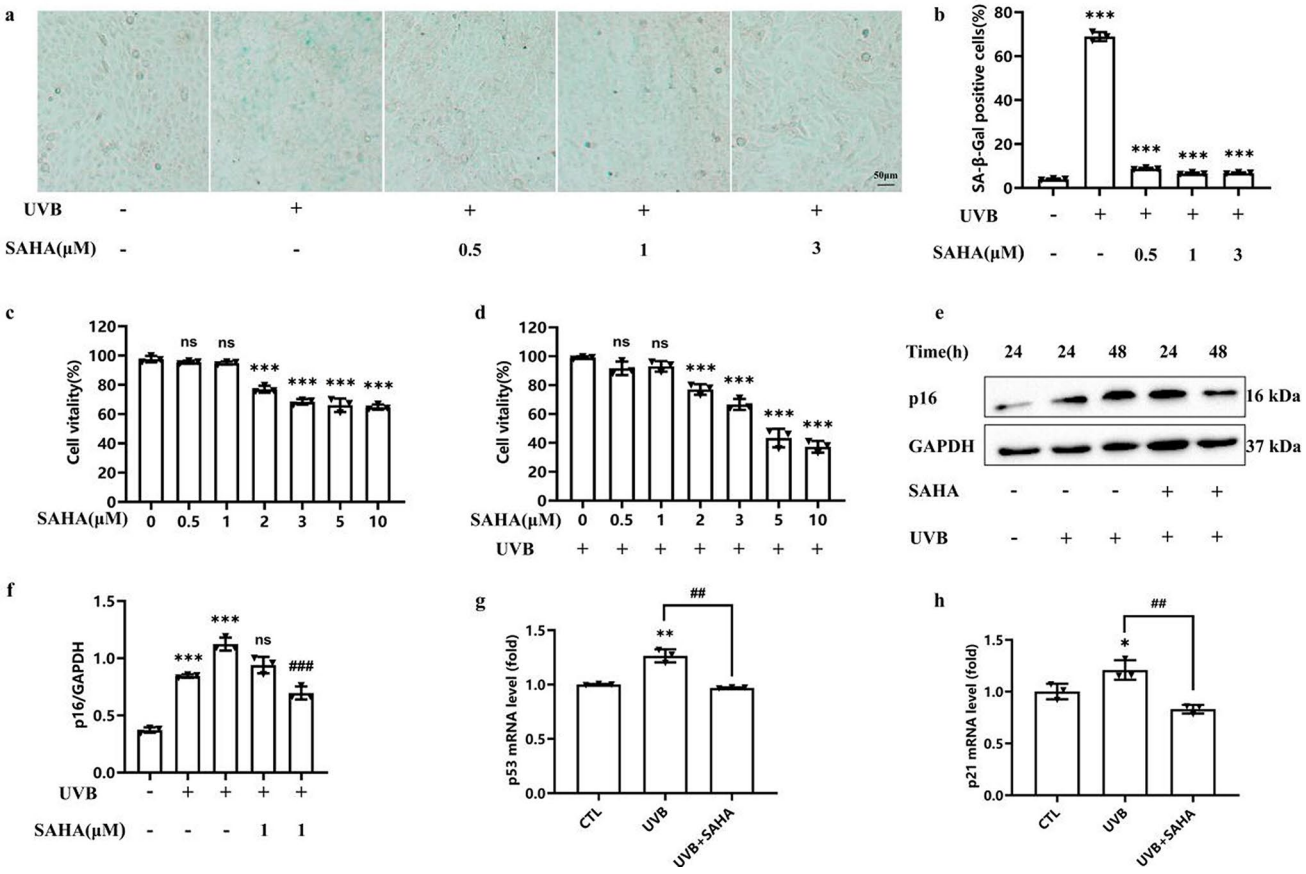

Fig. 1. SAHA alleviated UVB-induced senescence in HaCaT cells. (**a**,**b**) Images and percentages of SA-Gal-positive treated with plus various vorinostat concentrations in 48 h. n = 3 biological replicates for each group. (Scale bar: 50 μm). (**c**) Effect of SAHA on the viability of HaCaT cells. n = 3 biological replicates for each group. (**d**) Effect of SAHA on the viability of HaCaT cells after UVB irradiation. n = 3 biological replicates for each group. (**e**) p16, and GAPDH protein levels of HaCaT treated with UVB irradiation plus 1 μM SAHA in Days 1 and 2. n = 3 biological replicates for each group. (**f**) Relative protein level ratio of p16/GAPDH. (**g**,**h**) mRNA expression of p53, p21,18S and GAPDH of UVB irradiation and in combination with 1 μM SAHA were measured by RT-qPCR in 48 h. n = 3 biological replicates for each group. The data was expressed as mean ± SD, $^{*}p < 0.05$, $^{**}p < 0.01$, and $^{***}p < 0.001$. CTL: the control group; UVB: the model group; UVB + SAHA: the treatment group. −: untreated; +: treatment.

group, the expression level of p-NF-κB was significantly reduced compared to the UVB group (Fig. 3a,b). Subsequently, we examined the expression of downstream inflammatory factors in the NF-κB signaling pathway. The results showed that, compared to the control group, the levels of IL-1β, IL-6, IL-8, MCP-1, and TNF-α were significantly elevated in the UVB group. In contrast, the mRNA levels of these five inflammatory factors returned to normal following SAHA treatment (Fig. 3c–g). Collectively, these findings suggest that SAHA can mitigate UVB-induced photoaging by inhibiting the NF-κB signaling pathway.

SAHA can inhibit UVB-induced photoaging in mouse skin

We have confirmed that SAHA can alleviate UVB-induced senescence in HaCaT cells. To evaluate whether SAHA has an effect on reducing UVB-induced photoaging in vivo, we established a skin damage model in BALB/c mice using UVB radiation. The results indicated that, compared to the control group, mice in the UVB group developed noticeable erythema and scarring on their backs after UVB exposure. In contrast, the SAHA-treated group showed accelerated skin recovery and reduced skin damage compared to the UVB group (Fig. 4a). Additionally, we performed H&E staining on the back skin of BALB/c mice to further assess skin damage. We observed that after UVB exposure, the epidermal layer of the back skin in BALB/c mice was significantly thickened, and inflammatory factors were markedly increased. Following SAHA treatment, the symptoms of epidermal thickening and increased inflammatory factors were effectively improved (Fig. 4b,c). Subsequently, we performed senescence staining on frozen sections of mouse back skin. The results showed that the skin tissue in the UVB group exhibited intense blue staining, while the blue staining in the SAHA-treated and control groups was reduced (Fig. 4d). Additionally, we investigated the protein expression of p16 and the mTOR signaling pathway in the skin. The UVB group showed higher levels of p16 and mTOR protein expression compared to the control group, while SAHA significantly reduced the elevated expression of these proteins triggered by UVB

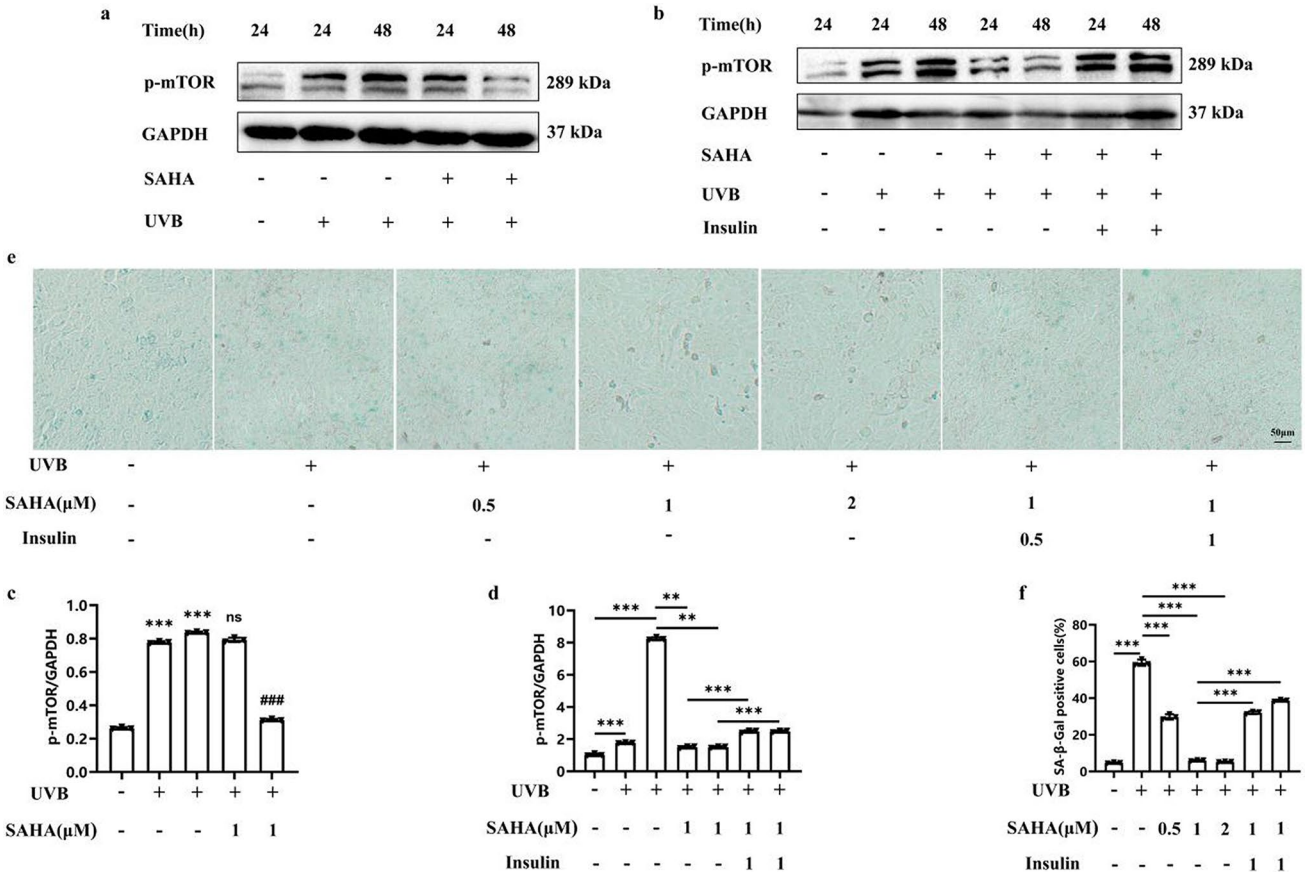

Fig. 2. SAHA inhibits the UVB-induced mTOR signaling pathways. (**a**) HaCaT treated with UVB irradiation plus 1 μM SAHA in Days 1 and 2. Representative images of immunoblotting of p-mTOR, and GAPDH. n = 3 biological replicates for each group. (**c**) Relative protein level ratio of p-mTOR/GAPDH. (**b**) HaCaT treated with UVB irradiation or plus 1 μM SAHA or notand insulin or not for 1 and 2 days. Representative images of immunoblotting of p-mTOR, and GAPDH. n = 3 biological replicates for each group. (**d**) Relative protein level ratio of p-mTOR/GAPDH. (**e**,**f**) SA-β-Gal positive representative images and statistical charts of HaCaT after different concentrations of drug in 48 h (Scale bar: 50 μm). The data was expressed as mean ± SD, $^{*}p < 0.05$, $^{**}p < 0.01$, and $^{***}p < 0.001$. CTL: the control group; UVB: the model group; UVB + SAHA: the treatment group. −: untreated; +: treatment.

(Fig. 4e–g). Our study demonstrates that SAHA can mitigate UVB-induced skin damage and alleviate UVB-induced photoaging of the skin tissue.

SAHA treatment alleviates UV-B-induced collagen fiber damage in skin tissue

Studies have shown that UVB primarily degrades type I collagen and inhibits its synthesis by upregulating the expression of matrix metalloproteinases (MMPs) such as collagenase (MMP-1), matrix metalloproteinase-3 (MMP-3), and gelatinase (MMP-9). Therefore, we assessed the protein expression of MMPs in HaCaT cells using Western blotting. The results indicated that, compared to the control group, the expression levels of MMP-1, MMP-3, and MMP-9 were significantly elevated at 48 h in the UVB group. In contrast, the expression levels of MMP-1, MMP-3, and MMP-9 were significantly reduced at 48 h in the SAHA-treated group compared to the UVB group (Fig. 5a–d). Subsequently, we observed collagen fiber arrangement in skin tissue using Masson's staining. We found that collagen fibers were organized in a well-aligned manner in the SAHA-treated group. However, under UVB exposure, collagen fibers in the skin tissue were significantly reduced compared to the SAHA group, indicating collagen degradation (Fig. 5e,f). Additionally, we assessed the protein expression of MMPs in mouse skin tissue. Consistent with the in vitro results, MMP-9 levels increased after UVB irradiation, and this increase was reversed by SAHA treatment (Fig. 5g,h). The results indicate that SAHA can inhibit the upregulation of expression of MMPs protein induced by UVB in both cells and mice, and alleviate the reduction of collagen fibers in UVB-exposed mouse skin.

Discussion

This study aims to elucidate the effects of SAHA on UVB-induced HaCaT cell and skin aging, as well as its underlying molecular mechanisms, to validate SAHA as an effective anti-senescence skin agent. Our findings demonstrate that SAHA significantly alleviates UVB-induced photoaging in HaCaT cells and mouse skin

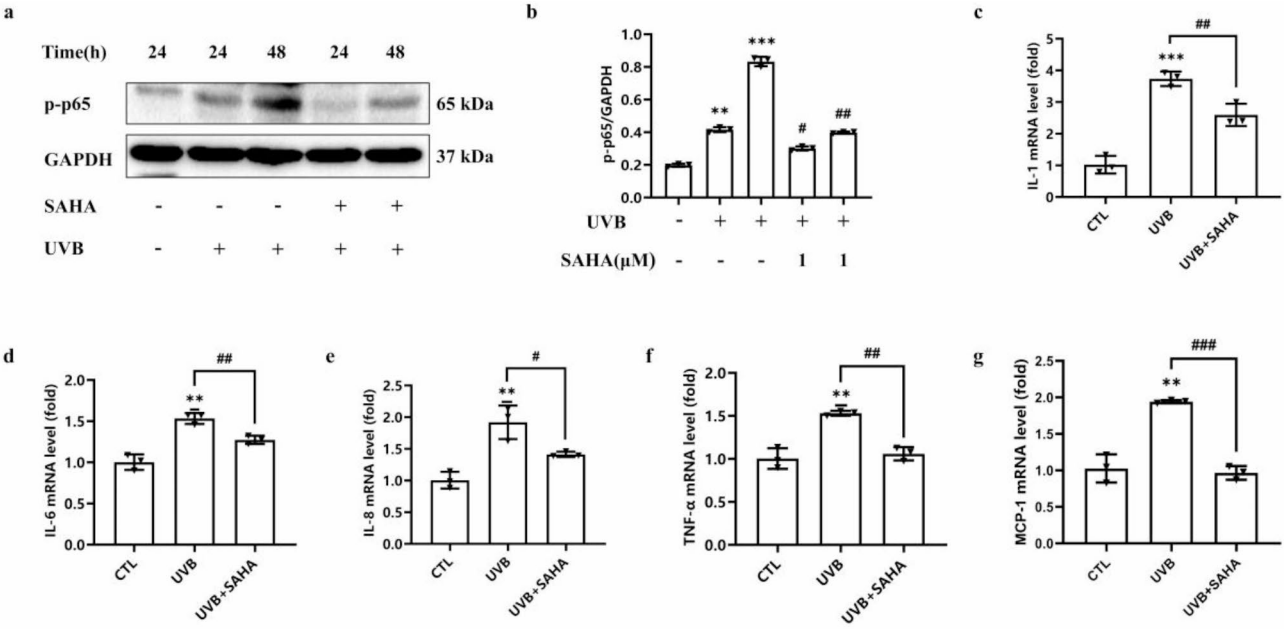

Fig. 3. SAHA inhibit UVB-induced inflammatory responses in HaCaT cells. (**a**) Western blotting of p-p65 and GAPDH protein levels in HaCaT cells treated with UVB irradiation plus 1 μM vorinostat or not on Days 1 and 2. n = 3 biological replicates for each group. (**b**) Relative protein level ratio of p-p65/GAPDH. (**c**)–(**g**) Relative gene expression was normalized to that of GAPDH or 18 s, and the genes IL-1β, IL-6, IL-8, MCP-1 and TNF-α as detected by RT-qPCR in 48 h. n = 3 biological replicates for each group. The data was expressed as mean ± SD, $^{*}p < 0.05$, $^{**}p < 0.01$, and $^{***}p < 0.001$. CTL: the control group; UVB: the model group; UVB + SAHA: the treatment group. −: untreated; +: treatment.

by modulating the NF-κB and mTOR signaling pathways, providing an alternative strategy for combating exogenous skin aging. Specifically, SAHA treatment significantly reduced senescence-associated β-galactosidase (SA-β-gal) activity, downregulated the expression of key senescence markers such as p16 and p21, and mitigated UVB-induced inflammatory responses by inhibiting the expression of pro-inflammatory cytokines including IL-1β, IL-6, and TNF-α. Histological analysis further revealed that SAHA preserved skin structural integrity by reducing epidermal thickening and preventing collagen degradation, indicating its protective effect on the skin through the downregulation of matrix metalloproteinases (MMP-1, MMP-3, and MMP-9). These results suggest that SAHA exerts its protective effects against UVB-induced photoaging by modulating key molecular pathways associated with senescence and inflammation, highlighting its potential as a therapeutic intervention to prevent and ameliorate skin aging.

Notably, the selection of UVB irradiation intensities for both in vivo and in vitro models was based on our prior research experience and extensive preliminary experiments conducted before the formal study[20,34]. These preliminary studies allowed us to optimize UVB parameters, ensuring the reproducibility and reliability of the photoaging model. In the in vitro model, HaCaT keratinocytes were exposed to 40 mJ/cm^2 and 50 mJ/cm^2 UVB. This dose range has been widely validated in multiple studies and is capable of effectively inducing key photoaging characteristics, including increased senescence-associated β-galactosidase (SA-β-gal) activity, upregulation of matrix metalloproteinases (MMPs), and DNA damage[38,39]. Moreover, this dose range ensures the induction of cellular senescence without excessive cytotoxicity, thereby preserving the feasibility of subsequent molecular mechanism analyses. In contrast, in vivo experiments required a significantly higher UVB dose of 750 mJ/cm^2 due to the intrinsic photoprotective properties of intact skin tissue. Specifically, the stratum corneum acts as a protective barrier that partially absorbs and scatters UVB, reducing its penetration depth[37]. Therefore, to achieve a photoaging phenotype in BALB/c mice comparable to that observed in vitro, we selected 750 mJ/cm^2 UVB irradiation. Our prior research have demonstrated that UVB doses 750 mJ/cm^2 effectively induce hallmark photoaging features in murine skin, such as epidermal thickening, dermal collagen degradation, enhanced oxidative stress, and increased pro-inflammatory cytokine expression[20,34]. We determined 750 mJ/cm^2 as the optimal dose to ensure successful induction of photoaging while minimizing tissue necrosis or irreversible damage. To further enhance the clinical relevance of this study, future research should explore chronic UVB exposure models in mice to better simulate long-term photodamage. Additionally, incorporating human skin organoid models or ex vivo skin cultures could more accurately replicate the three-dimensional microenvironment of the skin in vitro, thereby bridging the gap between monolayer cell cultures and whole-animal models.

Upon exposure to UVB radiation, DNA damage occurs within epidermal cells, leading to the activation of complex repair mechanisms[40]. These mechanisms are responsible for detecting and eliminating UVB-induced DNA damage, such as thymine dimers, to prevent the accumulation of genetic abnormalities[41]. Effective DNA

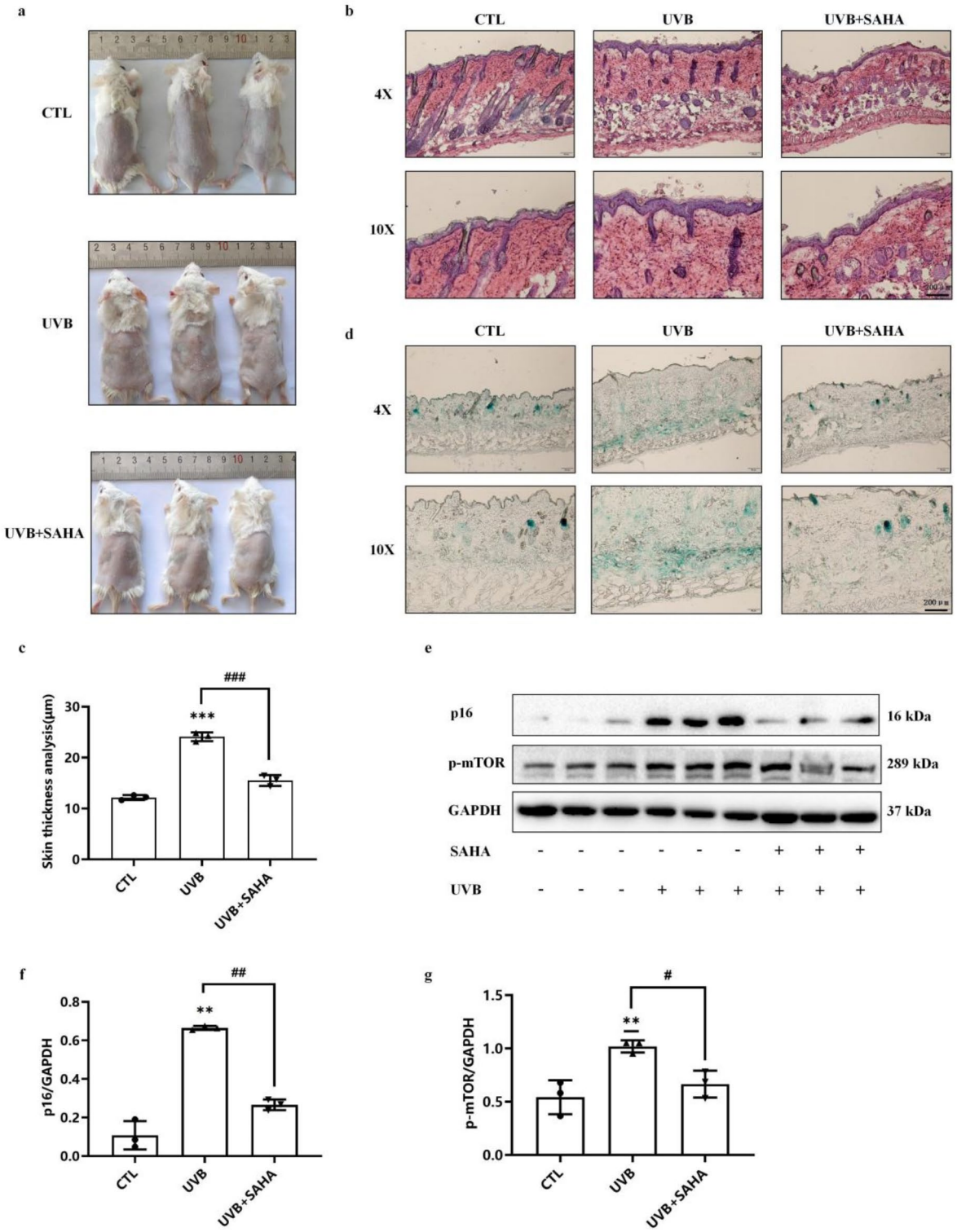

Fig. 4. SAHA can inhibit UVB-induced photoaging in mouse skin. (**a**) The images of the back of BALB/C mice. n = 6 biological replicates for each group. (**b**) HE staining (Magnification: 100× and 200×. Scale bars: 200 μm). (**c**) Skin thickness analysis. (**d**) SA-β-Gal staining of each group of tissues (Magnification: 100× and 200×. Scale bars: 200 μm). (**e**) Representative images from p16, p-mTOR, and GAPDH Western blot assays. n = 3 biological replicates for each group. (**f**,**g**) Quantification of relative protein levels. The data was expressed as mean ± SD, $^{*}p < 0.05$, $^{**}p < 0.01$, and $^{***}p < 0.001$. CTL: the control group; UVB: the model group; UVB + SAHA: the treatment group. −: untreated; +: treatment.

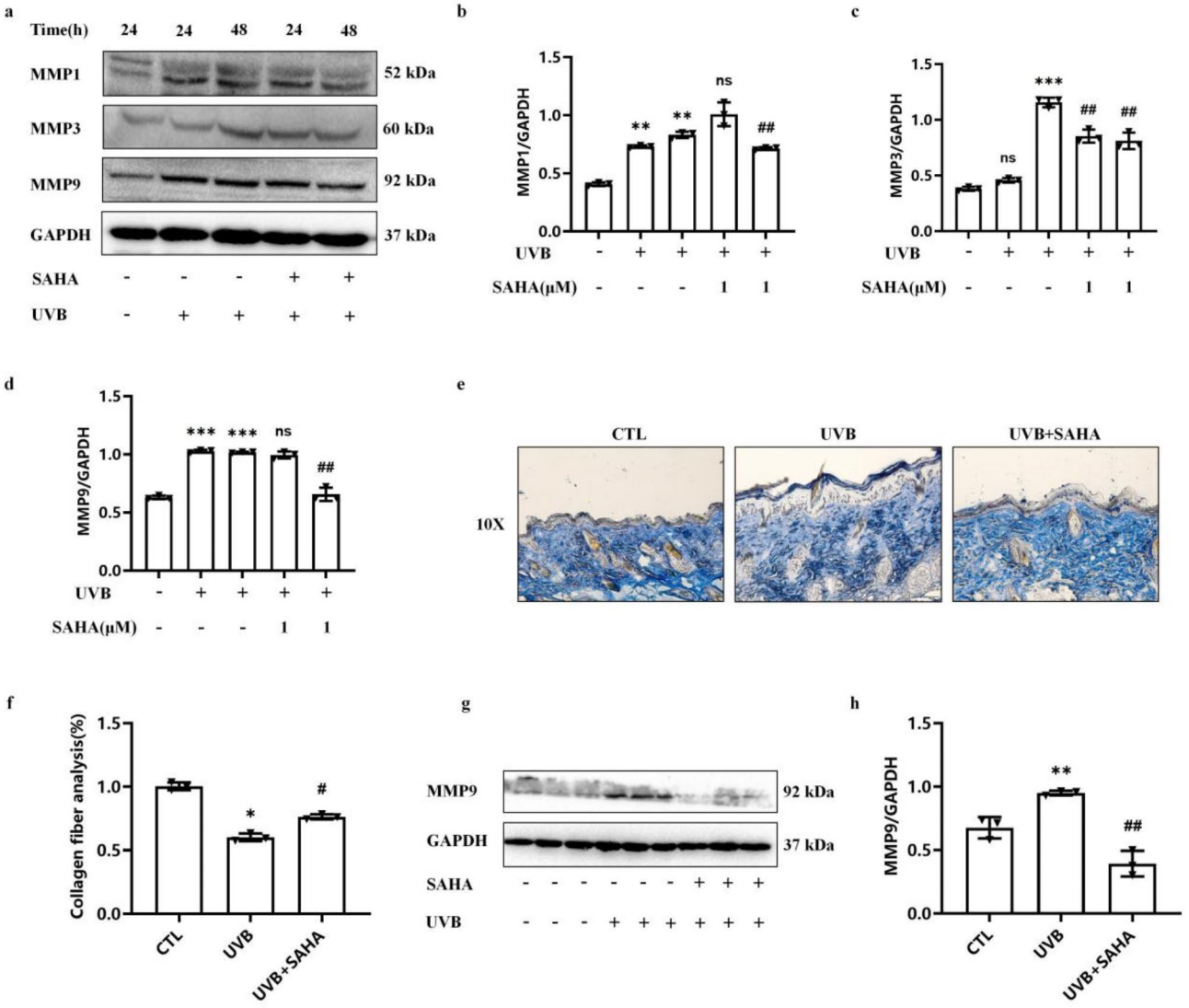

Fig. 5. SAHA treatment alleviates UVB-induced collagen fiber damage in skin tissue. (**a**)–(**d**) Representative images from MMP1, MMP3, MMP9, and GAPDH Western blot assays in Hacat cells treated with UVB irradiation plus 1 μM vorinostat or not on Days 1 and 2. n = 3 biological replicates for each group. (**e**) The images of Masson staining. (Magnification: 200×. Scale bars: 200 μm). (**f**) Collagen fiber analysis. (**g**) Representative images from MMP9, and GAPDH Western blot assays in mice. n = 3 biological replicates for each group. (**h**) Quantification of relative protein levels. The data was expressed as mean ± SD, $^{*}p < 0.05$, $^{**}p < 0.01$, and $^{***}p < 0.001$. CTL: the control group; UVB: the model group; UVB + SAHA: the treatment group. −: untreated; +: treatment.

repair is crucial for maintaining the integrity and function of epidermal cells. UVB radiation also triggers a series of responses in epidermal cells as protective mechanisms against photodamage. These responses include the activation of inflammation, oxidative stress, and senescence-associated cellular pathways, aimed at mitigating the harmful effects of UVB exposure and promoting cell survival. However, prolonged or excessive UVB exposure may overwhelm these protective mechanisms, leading to the accumulation of damage and the onset of photoaging[41]. Our study demonstrates that under UVB radiation, the accumulation of senescent cells increases in HaCaT cells and mouse skin, further triggering the process of photoaging. However, supplementation with SAHA can effectively alleviate cellular senescence and inhibit UVB-induced photoaging. Therefore, repairing and recovering from UVB-induced epidermal cell damage is necessary. Effective repair mechanisms can ensure the restoration of cellular homeostasis and prevent further deterioration of skin health.

UVB radiation-induced skin senescence involves a complex molecular cascade, including key signaling molecules such as Activator Protein-1 (AP-1), NF-κB, and autophagy. The NF-κB signaling pathway plays a crucial role in the inflammatory response, inducing the production of the inflammatory enzyme Cyclooxygenase-2 (COX-2) and the release of inflammatory cytokines. The increase in these pro-inflammatory cytokines further stimulates the production of ROS, creating a vicious cycle that damages skin tissue cells and induces their excessive secretion of matrix metalloproteinases (MMPs), leading to collagen degradation and skin photoaging[42].

Therefore, anti-inflammatory approaches may be an effective therapeutic strategy to prevent UVB-induced skin senescence. Autophagy is a crucial lysosomal degradation mechanism that maintains cytoplasmic quality by eliminating protein aggregates and damaged organelles[8]. The regulation of autophagy involves a complex signaling network, including mTOR and AMPK pathways, which modulate senescence and lifespan[25,43]. In this study, we found that the application of SAHA significantly reduced the expression of pro-inflammatory factors such as TNF-α, IL-6, IL-8, IL-1, and MCP-1 in human keratinocytes. Western blot results showed that UVB radiation activated the NF-κB and mTOR signaling pathways, while SAHA supplementation effectively inhibited the expression of NF-κB and mTOR. Interestingly, when we added the mTOR activator insulin, the therapeutic effects of SAHA were attenuated. This indicates that the mTOR pathway plays a crucial role in the mechanism of action of SAHA. Recent studies have also shown that UVB can activate the mTORC2/Akt/IKKα signaling cascade, enhancing NF-κB activation[44], which is consistent with our findings. These results suggest that the application of SAHA may help repair UVB-induced skin photoaging damage mediated by inflammation and senescence by inhibiting the harmful NF-κB and mTOR signaling pathways. Thus, SAHA could be a potential therapeutic strategy for UVB-induced skin senescence.

A prominent feature of photoaging is the decrease in collagen content within the skin, a process regulated by various complex signaling pathways[45,46]. Collagen is a key substance that maintains skin softness and firmness, but its levels gradually decline with senescence[8,47]. UVB exposure increases the expression of matrix metalloproteinases (MMPs) in the skin. MMPs are zinc-containing endopeptidases responsible for degrading extracellular matrix (ECM) proteins, such as collagen, fibronectin, elastin, and proteoglycans, which is a major cause of photoaging[48]. MMPs, including MMP-1, MMP-9, and MMP-6, play important roles in normal physiological processes, but their dysregulation is closely associated with skin senescence[49]. Therefore, inhibiting MMP activity can mitigate UV-induced photoaging. In this study, we found that SAHA treatment significantly reduced the UVB-induced upregulation of MMP-1, MMP-9, and MMP-6, thereby preventing excessive collagen degradation and slowing the skin senescence process. Additionally, prolonged UV exposure increases the thickness of the skin epidermis, and the rupture of collagen fibers leads to weakened skin structure[1,50]. Our research indicates that SAHA supplementation not only alleviates epidermal thickening but also increases the number of elastic fibers, resulting in a more ordered and compact arrangement of collagen fibers, thereby maintaining the structural integrity of the skin. These findings strongly suggest that SAHA has the potential to promote the repair of photoaged cells and slow collagen degradation. By modulating MMP expression levels, SAHA offers a promising therapeutic approach for improving UV-induced photoaging.

SAHA has been extensively studied in dermatological conditions, such as cutaneous T-cell lymphoma, melanoma, and psoriasis. In the treatment of cutaneous T-cell lymphoma, SAHA has demonstrated clinical efficacy in malignant cutaneous T-cell lymphoma cell lines isolated from patients. Additionally, the combination of SAHA and quercetin significantly enhanced apoptosis in cutaneous T-cell lymphoma[51,52]. These findings demonstrate the potential efficacy of SAHA for skin conditions. Interestingly, our study demonstrates that SAHA exhibits effective therapeutic effects in UVB-induced photoaging models of HaCaT cells and mouse skin. Additionally, in keratinocytes (KCs), SAHA reduces psoriatic-like features, decreases epidermal thickness, and inhibits epidermal proliferation[53]. In our study, we found that SAHA effectively alleviated UVB-induced damage, accelerated the recovery of damaged skin, and reduced epidermal thickness, consistent with the above findings. Therefore, our research provides a new strategy for alleviating UVB-induced photoaging through the anti-senescence agent SAHA.

The current research aims to investigate the potential of SAHA in alleviating UVB-induced photoaging in HaCaT cells and mouse skin. Our data indicate that SAHA effectively mitigates UVB-induced cellular and skin senescence phenomena, with a significant improvement in photoaging. Specifically, SAHA appears to exert its therapeutic effects by inhibiting the NF-κB and mTOR signaling pathways. This suggests that SAHA may be a potential tool for controlling UVB-induced photoaging. However, despite SAHA's demonstrated benefits, there are some limitations to consider. While inhibiting NF-κB and mTOR signaling pathways is beneficial for alleviating UVB-induced photoaging, senescence is regulated by a complex network of signals, including telomere loss, epigenetic changes, protein homeostasis disruption, and stem cell depletion. Therefore, relying solely on the inhibition of specific signaling pathways may not be sufficient to comprehensively address photoaging. Future research should further explore the specific mechanisms of SAHA in the treatment of UVB-induced photoaging, particularly its effects on other senescence-related signaling networks. Additionally, investigating how to optimize SAHA's application for more comprehensive anti-senescence effects is an important direction for future studies.

Another important consideration in this study is that UVB-induced skin photoaging is a rapidly progressing process, and our research primarily focuses on evaluating the intervention effects of SAHA during the early stages of UVB-induced photoaging. We chose 6 days as the experimental time point because, within a short period after UVB exposure, the skin exhibits significant acute damage responses, such as the activation of aging markers and the initiation of inflammatory responses. According to literature reports, these early changes usually reach their peak within 24 h to 1 week post-UVB exposure, making 6 days an ideal time window to effectively assess the initial regulatory effect of SAHA on UVB-induced skin photoaging[20,54–56]. Additionally, we only observed the impact of SAHA on UVB-induced mouse skin photoaging with a 6-day window because, during the experiment, we observed that the skin tissue on the back of the mice had largely recovered by day six. Therefore, we did not extend the SAHA treatment duration further. However, we recognize that the long-term and complex nature of anti-aging effects means that short-term experiments may not fully reflect the comprehensive impact of the intervention throughout the aging process. Although we observed significant physiological and molecular-level changes in the short term, aging is a multi-dimensional and progressive biological process, involving cellular damage, gene expression regulation, tissue degeneration, and other aspects[57,58]. Consequently, based on our current experimental design, the results may only reflect the intervention effects at the early stages and cannot fully reveal the long-term impact of treatment on the aging process. To address this limitation, we suggest that future research extend the observation period to explore the long-term effects and mechanisms of anti-aging interventions. For example, a 6-month

or longer animal experimental cycle could be used to more comprehensively evaluate the lasting impact of the intervention on aging-related physiology, tissue structure, cellular functions, and molecular biomarkers. Moreover, long-term experiments will also help verify whether the anti-aging effects we have currently observed can resist ongoing internal and external environmental stressors (such as chronic oxidative stress and inflammation), which are considered to play key roles in the aging process[25,59]. We believe that extending the experimental duration will provide more comprehensive data, helping us understand the persistence and sustainability of anti-aging interventions at both the physiological and molecular levels.

This study aims to elucidate the effects and molecular mechanisms of SAHA on UVB-induced HaCaT cell and skin senescence, in order to validate SAHA as an effective anti-senescence agent for the skin. Our findings indicate that SAHA effectively alleviates UVB-induced photoaging in HaCaT cells and mouse skin through the NF-κB and mTOR signaling pathways, providing an alternative strategy for addressing exogenous skin senescence.

Data availability

The datasets used and/or analysed during the current study available from the corresponding author on reasonable request.

Received: 12 August 2024; Accepted: 24 March 2025
Published online: 29 March 2025

References

1. Zhu, S. et al. The nanostructured lipid carrier gel of Oroxylin A reduced UV-induced skin oxidative stress damage. *Colloids Surf. B Biointerfaces* **216**, 112578. https://doi.org/10.1016/j.colsurfb.2022.112578 (2022).
2. Wang, L., Je, J. G., Yang, H. W., Jeon, Y. J. & Lee, S. Dieckol, an algae-derived phenolic compound, suppresses UVB-induced skin damage in human dermal fibroblasts and its underlying mechanisms. *Antioxidants (Basel)* **10**, 352. https://doi.org/10.3390/antiox10030352 (2021).
3. Wang, L., Oh, J. Y., Lee, W. & Jeon, Y. J. Fucoidan isolated from *Hizikia fusiforme* suppresses ultraviolet B-induced photodamage by down-regulating the expressions of matrix metalloproteinases and pro-inflammatory cytokines via inhibiting NF-kappaB, AP-1, and MAPK signaling pathways. *Int. J. Biol. Macromol.* **166**, 751–759. https://doi.org/10.1016/j.ijbiomac.2020.10.232 (2021).
4. Wang, L. et al. Anti-photoaging and anti-melanogenesis effects of fucoidan isolated from *Hizikia fusiforme* and its underlying mechanisms. *Mar. Drugs* **18**, 427. https://doi.org/10.3390/md18080427 (2020).
5. Garcia-Gil, S. et al. Photoprotective effects of two new Morin-Schiff base derivatives on UVB-irradiated HaCaT cells. *Antioxidants (Basel)* **13**, 134. https://doi.org/10.3390/antiox13010134 (2024).
6. Long, Y. et al. Photoprotective effects of *Dendrobium nobile* Lindl. polysaccharides against UVB-induced oxidative stress and apoptosis in HaCaT cells. *Int. J. Mol. Sci.* **24**, 6120. https://doi.org/10.3390/ijms24076120 (2023).
7. Chen, Y. et al. *Premna microphylla* Turcz pectin protected UVB-induced skin aging in BALB/c-nu mice via Nrf2 pathway. *Int. J. Biol. Macromol.* **215**, 12–22. https://doi.org/10.1016/j.ijbiomac.2022.06.076 (2022).
8. Kim, C. W. et al. gamma-Mangosteen, an autophagy enhancer, prevents skin-aging via activating KEAP1/NRF2 signaling and downregulating MAPKs/AP-1/NF-kappaB-mediated MMPs. *Phytomedicine* **132**, 155815. https://doi.org/10.1016/j.phymed.2024.155815 (2024).
9. Yoshimura, T. et al. Protective effect of taurine on UVB-induced skin aging in hairless mice. *Biomed. Pharmacother.* **141**, 111898. https://doi.org/10.1016/j.biopha.2021.111898 (2021).
10. Zhao, Y., Simon, M., Seluanov, A. & Gorbunova, V. DNA damage and repair in age-related inflammation. *Nat. Rev. Immunol.* **23**, 75–89. https://doi.org/10.1038/s41577-022-00751-y (2023).
11. Gu, Y., Han, J., Jiang, C. & Zhang, Y. Biomarkers, oxidative stress and autophagy in skin aging. *Ageing Res. Rev.* **59**, 101036. https://doi.org/10.1016/j.arr.2020.101036 (2020).
12. Xie, Y. et al. Damage prevention effect of milk-derived peptides on UVB irradiated human foreskin fibroblasts and regulation of photoaging related indicators. *Food Res. Int.* **161**, 111798. https://doi.org/10.1016/j.foodres.2022.111798 (2022).
13. Park, J. Y., Lee, J., Kim, Y. & Kang, C. H. *Latilactobacillus sakei* Wikim0066 protects skin through MMP regulation on UVB-irradiated in vitro and in vivo model. *Nutrients* **15**, 726. https://doi.org/10.3390/nu15030726 (2023).
14. Lee, E. S. et al. Sarmentosamide, an anti-aging compound from a marine-derived *Streptomyces* sp. APmarine042. *Mar. Drugs* **18**, 463. https://doi.org/10.3390/md18090463 (2020).
15. Matsumura, Y. & Ananthaswamy, H. N. Toxic effects of ultraviolet radiation on the skin. *Toxicol. Appl. Pharmacol.* **195**, 298–308. https://doi.org/10.1016/j.taap.2003.08.019 (2004).
16. Kim, J. et al. Krill oil's protective benefits against ultraviolet B-induced skin photoaging in hairless mice and in vitro experiments. *Mar. Drugs* **21**(9), 479. https://doi.org/10.3390/md21090479 (2023).
17. Seol, J. E. et al. Echinochrome a protects against ultraviolet B-induced photoaging by lowering collagen degradation and inflammatory cell infiltration in hairless mice. *Mar. Drugs* **19**, 550. https://doi.org/10.3390/md19100550 (2021).
18. Vousden, K. H. & Lane, D. P. p53 in health and disease. *Nat. Rev. Mol. Cell Biol.* **8**, 275–283. https://doi.org/10.1038/nrm2147 (2007).
19. Harper, J. W. et al. The p21 Cdk-interacting protein Cip1 is a potent inhibitor of G1 cyclin-dependent kinases. *Cell* **75**(4), 805–816. https://doi.org/10.1016/0092-8674(93)90499-g (1993).
20. Ge, Y. et al. Doxercalciferol alleviates UVB-induced HaCaT cell senescence and skin photoaging. *Int. Immunopharmacol.* **127**, 111357. https://doi.org/10.1016/j.intimp.2023.111357 (2024).
21. Campisi, J. & Robert, L. Cell senescence: Role in aging and age-related diseases. *Interdiscip. Top. Gerontol.* **39**, 45–61. https://doi.org/10.1159/000358899 (2014).
22. Zhang, Y., Huang, S., Xie, B. & Zhong, Y. Aging, cellular senescence, and glaucoma. *Aging Dis.* **15**, 546–564. https://doi.org/10.14336/AD.2023.0630-1 (2024).
23. Zinger, A., Cho, W. C. & Ben-Yehuda, A. Cancer and aging—The inflammatory connection. *Aging Dis.* **8**, 611–627. https://doi.org/10.14336/AD.2016.1230 (2017).
24. Xia, J. et al. Metformin ameliorates 5-fluorouracil-induced intestinalinjury by inhibiting cellular senescence, inflammation, and oxidative stress. *Int. Immunopharmacol.* **113**, 109342. https://doi.org/10.1016/j.intimp.2022.109342 (2022).
25. Jia, H. J. et al. Trifluridine induces HUVECs senescence by inhibiting mTOR-dependent autophagy. *Biochem. Biophys. Res. Commun.* **610**, 119–126. https://doi.org/10.1016/j.bbrc.2022.04.063 (2022).
26. Kim, D. J., Iwasaki, A., Chien, A. L. & Kang, S. UVB-mediated DNA damage induces matrix metalloproteinases to promote photoaging in an AhR- and SP1-dependent manner. *JCI Insight* **7**, e156344. https://doi.org/10.1172/jci.insight.156344 (2022).
27. Wang, Y. et al. Anti-photoaging effects of flexible nanoliposomes encapsulated *Moringa oleifera* Lam. isothiocyanate in UVB-induced cell damage in HaCaT cells. *Drug Deliv.* **29**, 871–881. https://doi.org/10.1080/10717544.2022.2039802 (2022).

28. Thapa Magar, T. B. et al. Chlorin E6-curcumin-mediated photodynamic therapy promotes an anti-photoaging effect in UVB-irradiated fibroblasts. *Int. J. Mol. Sci.* **24**, 13468. https://doi.org/10.3390/ijms241713468 (2023).
29. Hu, J. et al. Structural characterization and anti-photoaging activity of a polysaccharide from *Sargassum fusiforme*. *Food Res. Int.* **157**, 111267. https://doi.org/10.1016/j.foodres.2022.111267 (2022).
30. Marks, P. et al. Histone deacetylases and cancer: Causes and therapies. *Nat. Rev. Cancer* **1**(3), 194–202. https://doi.org/10.1038/35106079 (2001).
31. Duvic, M. et al. Phase 2 trial of oral vorinostat (suberoylanilide hydroxamic acid, SAHA) for refractory cutaneous T-cell lymphoma (CTCL). *Blood* **109**, 31–39. https://doi.org/10.1182/blood-2006-06-025999 (2007).
32. Ma, W. et al. Sensitizing triple negative breast cancer to tamoxifen chemotherapy via a redox-responsive vorinostat-containing polymeric prodrug nanocarrier. *Theranostics* **10**, 2463–2478. https://doi.org/10.7150/thno.38973 (2020).
33. Pun, M. D. et al. Phosphorus containing analogues of SAHA as inhibitors of HDACs. *J. Enzyme Inhib. Med. Chem.* **37**(1), 1315–1319. https://doi.org/10.1080/14756366.2022.2063281 (2022).
34. Jia, H. J., Ge, Y., Xia, J., Shi, Y. L. & Wang, X. B. Belinostat (PXD101) resists UVB irradiation-induced cellular senescence and skin photoaging. *Biochem. Biophys. Res. Commun.* **627**, 122–129. https://doi.org/10.1016/j.bbrc.2022.08.038 (2022).
35. Truong, V. L., Bae, Y. J., Bang, J. H. & Jeong, W. S. Combination of red ginseng and velvet antler extracts prevents skin damage by enhancing the antioxidant defense system and inhibiting MAPK/AP-1/NF-kappaB and caspase signaling pathways in UVB-irradiated HaCaT keratinocytes and SKH-1 hairless mice. *J. Ginseng. Res.* **48**, 323–332. https://doi.org/10.1016/j.jgr.2024.01.003 (2024).
36. Zhang, H. et al. Human adipose and umbilical cord mesenchymal stem cell-derived extracellular vesicles mitigate photoaging via TIMP1/Notch1. *Signal Transduct. Target Ther.* **9**, 294. https://doi.org/10.1038/s41392-024-01993-z (2024).
37. Li, Z. et al. Ginsenosides repair UVB-induced skin barrier damage in BALB/c hairless mice and HaCaT keratinocytes. *J. Ginseng. Res.* **46**, 115–125. https://doi.org/10.1016/j.jgr.2021.05.001 (2022).
38. Choi, S. I. et al. *Eisenia bicyclis* extract repairs UVB-induced skin photoaging in vitro and in vivo: Photoprotective effects. *Mar. Drugs* **19**, 693. https://doi.org/10.3390/md19120693 (2021).
39. de Gruijl, F. R. et al. UV-induced DNA damage, repair, mutations and oncogenic pathways in skin cancer. *J. Photochem. Photobiol. B* **63**, 1–3. https://doi.org/10.1016/s1011-1344(01)00199-3 (2001).
40. Lee, B. Y. et al. Senescence-associated beta-galactosidase is lysosomal beta-galactosidase. *Aging Cell* **5**, 187–195. https://doi.org/10.1111/j.1474-9726.2006.00199.x (2006).
41. Marabini, L. et al. Effects of *Vitis vinifera* L. leaves extract on UV radiation damage in human keratinocytes (HaCaT). *J Photochem. Photobiol. B* **204**, 111810. https://doi.org/10.1016/j.jphotobiol.2020.111810 (2020).
42. Zhu, S. et al. The nanostructured lipid carrier gel of Oroxylin A reduced UV-induced skin oxidative stress damage. *Colloids Surf. B Biointerfaces* **216**, 112578. https://doi.org/10.1016/j.ijbiomac.2022.06.076 (2022).
43. Xia, J. et al. Marimastat alleviates oxidative stress induced cellular senescence by activating autophagy. *Biochem. Biophys. Res. Commun.* **620**, 121–128. https://doi.org/10.1016/j.bbrc.2022.06.075 (2022).
44. Stoykova, I. D. et al. Myconoside and calceolarioside E restrain UV-induced skin photoaging by activating NRF2-mediated defense mechanisms. *Int. J. Mol. Sci.* **25**(4), 2441. https://doi.org/10.3390/ijms25042441 (2024).
45. Wu, P. Y. et al. 1,2-Bis[(3-methoxyphenyl)methyl]ethane-1,2-dicarboxylic acid reduces UVB-induced photodamage in vitro and in vivo. *Antioxidants (Basel)* **8**, 452. https://doi.org/10.3390/antiox8100452 (2019).
46. Chen, Y. et al. *Premna microphylla* Turcz pectin protected UVB-induced skin aging in BALB/c-nu mice via Nrf2 pathway. *Int. J. Biol. Macromol.* **215**, 12–22. https://doi.org/10.1016/j.ijbiomac.2022.06.076 (2022).
47. Park, J. Y., Lee, J. Y., Kim, Y. & Kang, C. H. *Latilactobacillus sakei* Wikim0066 protects skin through MMP regulation on UVB-irradiated in vitro and in vivo model. *Nutrients* **15**, 726. https://doi.org/10.3390/nu15030726 (2023).
48. Seol, J. E. et al. Echinochrome a protects against ultraviolet B-induced photoaging by lowering collagen degradation and inflammatory cell infiltration in hairless mice. *Mar. Drugs* **9**(10), 550. https://doi.org/10.3390/md19100550 (2021).
49. Xu, J. et al. Heat-killed *Lacticaseibacillus paracasei* ameliorated UVB-induced oxidative damage and photoaging and its underlying mechanisms. *Antioxidants (Basel)* **11**(10), 1875. https://doi.org/10.3390/antiox11101875 (2022).
50. Kim, J. A., Lee, J., Kim, J. H., Lee, H. J. & Kang, N. J. Penta-1,2,3,4,6-O-galloyl-β-D-glucose inhibits UVB-induced photoaging by targeting PAK1 and JNK1. *Antioxidants (Basel)* **8**(11), 561. https://doi.org/10.3390/antiox8110561 (2019).
51. Sidiropoulou, P. T. K. et al. New insights into granulomatous mycosis fungoides (GMF): A single-center experience. *Eur. J. Cancer* **156**, S69–S70 (2021).
52. Fujii, K., Idogawa, M., Suzuki, N., Iwatsuki, K. & Kanekura, T. Functional depletion of HSP72 by siRNA and quercetin enhances vorinostat-induced apoptosis in an HSP72-overexpressing cutaneous T-cell lymphoma cell line, Hut78. *Int. J. Mol. Sci.* **22**, 11258. https://doi.org/10.3390/ijms222011258 (2021).
53. Samuelov, L. et al. Vorinostat, a histone deacetylase inhibitor, as a potential novel treatment for psoriasis. *Exp. Dermatol.* **31**, 567–576. https://doi.org/10.1111/exd.14502 (2022).
54. Matsumura, Y. & Ananthaswamy, H. N. Short-term and long-term cellular and molecular events following UV irradiation of skin: Implications for molecular medicine. *Expert Rev. Mol. Med.* **4**(26), 1–22. https://doi.org/10.1017/S146239940200532X (2002).
55. Shime, H. et al. UVB irradiation expands skin-resident CD81(+)Foxp3(+) regulatory T cells with a highly activated phenotype. *J. Investig. Dermatol.* https://doi.org/10.1016/j.jid.2024.11.008 (2024).
56. Zhang, S., Chen, Y. & Qu, L. Protective effects of *Rosa roxburghii* Tratt. extract against UVB-induced inflammaging through inhibiting the IL-17 pathway. *Sci. Rep.* **15**, 8260. https://doi.org/10.1038/s41598-025-92559-8 (2025).
57. Gems, D. & de Magalhaes, J. P. The hoverfly and the wasp: A critique of the hallmarks of aging as a paradigm. *Ageing Res. Rev.* **70**, 101407. https://doi.org/10.1016/j.arr.2021.101407 (2021).
58. Wang, Z. et al. Network pharmacology and experimental verification revealing valnemulin alleviates DSS-induced ulcerative colitis by inhibiting intestinal senescence. *Int. Immunopharmacol.* **141**, 112810. https://doi.org/10.1016/j.intimp.2024.112810 (2024).
59. Sun, H. et al. Metformin protects 5-Fu-induced chemotherapy oral mucositis by reducing endoplasmic reticulum stress in mice. *Eur. J. Pharm. Sci.* **173**, 106182. https://doi.org/10.1016/j.ejps.2022.106182 (2022).

Acknowledgements

The Special Basic Cooperative Research Programs of Yunnan Provincial Undergraduate Universities' Association (Grant No. 202301BA070001-046) and (Grant No. 202401BA070001-071).

Author contributions

Qianlong Dai: Methodology, investigation, writing-original draft, conceptualization. Zhiwei Wang and Xue Wang: Methodology, investigation, writing—original draft, conceptualization. Wei Lian: Validation. Yuchen Ge: Investigation. Shujia Song: Validation. Fuxing Li: Investigation. Bingxiang Zhao and Lihua Li: Investigation. Xiaobo Wang, Jianjie Cheng, and Min Zhou: Writing-review and editing, supervision, methodology.

Declarations

Competing interests
The authors declare no competing interests.

Additional information
Supplementary Information The online version contains supplementary material available at https://doi.org/10.1038/s41598-025-95624-4.

Correspondence and requests for materials should be addressed to X.W., M.Z. or J.C.

Reprints and permissions information is available at www.nature.com/reprints.

Publisher's note Springer Nature remains neutral with regard to jurisdictional claims in published maps and institutional affiliations.